Table 3 Multivariate cox proportional hazards model analyses of various factors affecting overall survival in primary, resected stage IA NSCLC

Variable	Total			Male			Female		
	Hazard ratio	95% CI	P	Hazard ratio	95% CI	P	Hazard ratio	95% CI	P
Sex, male vs. female	1.422	1.179–1.715	0.0002	–	–	–	–	–	–
Age, ≥70 years vs. <70 years	1.548	1.325–1.808	<0.0001	1.605	1.333–1.605	<0.0001	1.470	1.106–1.470	0.0080
Performance status, ≥1 vs. 0	1.727	1.461–2.037	<0.0001	1.869	1.545–1.869	<0.0001	1.383	0.994–1.926	0.0543
Pack-years, ≥40 vs. <40	1.129	0.948–1.344	0.1742	1.148	0.955–1.379	0.1410	0.841	0.463–1.526	0.5697
Histologic type[a], squamous vs. nonsquamous	1.080	0.909–1.284	0.3807	1.168	0.973–1.401	0.0950	1.697	1.049–2.739	0.0309

[a] Nonsquamous cell carcinoma is comprised of adenocarcinoma and large cell carcinoma.

Table 4 Multivariate cox proportional hazards model analyses of various factors affecting disease-specific survival in primary, resected stage IA NSCLC

Variable	Total			Male			Female		
	Hazard ratio	95% CI	P	Hazard ratio	95% CI	P	Hazard ratio	95% CI	P
Sex, male vs. female	1.325	1.054–1.664	0.0161	–	–	–	–	–	–
Age, ≥70 years vs. <70 years	1.314	1.080–1.597	0.0063	1.350	1.068–1.706	0.0120	1.265	0.886–1.808	0.1949
Performance status, ≥1 vs. 0	1.387	1.119–1.718	0.0029	1.475	1.151–1.890	0.0022	1.088	0.705–1.680	0.7018
Pack-years, ≥40 vs. <40	1.218	0.981–1.511	0.0741	1.263	1.004–1.587	0.0463	0.768	0.351–1.675	0.5069
Histologic type[a], squamous vs. nonsquamous	1.098	0.886–1.360	0.3935	1.160	0.926–1.455	0.1971	1.517	0.810–2.849	0.1926

[a] Nonsquamous cell carcinoma is comprised of adenocarcinoma and large cell carcinoma.

ation between smoking history and lung cancer survival [17,18]; however, these studies did not utilize multivariate analysis. Harpole et al. reported a multivariate model that quantified the risk of recurrence and cancer death for patients with stage I NSCLC, but they demonstrated no significant impact on univariate analysis using smoking history [7]. Some other studies showed smoking history is negative prognostic factor [19,20]. However, their studies included relatively small cases and therefore may be insufficient power to detect smoking effects.

Hinds et al. reported model-predicted survival curves in women for smokers and never-smokers after adjustments for age, disease stage at diagnosis, and tumor histology [8]. The curves were significantly different. But, they did not use the Cox proportional hazards model and did not have information on pretreatment PS. Sobue et al. reported that current smokers who smoked 50 pack-years or more showed a 2.38 times higher risk of death than non-smokers for patients who undergo operations for adenocarcinoma of the lung [10]. Isobe et al. reported similar results [11]. In contrast, Sioris et al. showed that smoking history is one of the prognostic factors in squamous cell carcinoma for overall survival but not in adenocarcinoma [13]. Fujisawa et al. provided answer to this conflict. They employed multivariate analysis and showed smoking history is prognostic factor in evaluating overall long-term survival in patients with stage I primary resected NSCLC [14]. Nevertheless, they did not show important information on pretreatment PS. Furthermore, smoking history is not prognostic factor in evaluating disease-specific survival. It has been said that comorbidity may be one of the most important prognostic factor [22], as smoking is strongly associated with numerous serious disease such as chronic obstructive pulmonary disease, coronary heart disease, and stroke. To offset the influence of comorbidities on survival, disease-specific survival is superior to overall survival. On the other hand, the large number of patients at the multicenter gave us considerable confidence in the reliability of our data on smoking history and prognosis.

In our study, smoking status was investigated only at the time of admission to the hospital, and no information on smoking status was obtained after the operation. Richardson et al. reported that patients treated for SCLC who continue to smoke cigarettes increase their rate of developing second lung cancers [23]. In Japan, Kawahara et al. reported the same results [24]. In NSCLC, Fujisawa et al. reported no significant differences between postoperative smoking status and outcome in the population of patients, alive or dead, due to recurrent disease, second malignancy, or non-malignant disease [14]. Further study is necessary to determine the prognosis and incidence of recurrence among patients who continue to smoke.

Although the mechanisms by which smoking affects the prognosis of lung cancer patients independently of other factors are not yet clear, some recent reports on oncogene suggest the clinical influence of cigarette smoking. Molecular changes that have been demonstrated in lung cancer include the activation of oncogenes such as ras, myc, bcl-2, and c-erbB-2, and the loss of tumor suppressor genes such as p53, RB and $p16^{INK4\alpha}$ [25–27]. Recently, Vahakangas et al. reported that p53 mutations occur more commonly in smokers and ex-smokers than in never-smokers [28]. Furthermore, Tammemagi et al. reported that p53 alteration and smoking history are negative prognostic factor [15]. Heavy smokers may have these molecular changes. These reports support our data showing poor prognosis in heavy smokers.

Among patients with resectable tumors, advanced age is generally described as an unfavorable prognostic factor, possibly because of higher postoperative mortality rates [29]. Our findings confirmed that age is a prognostic factor in a curative resection setting.

Gender and smoking history were closely correlated in Japan. In this series, we observed striking differences in smoking history between men and women; that is, 82.5% of women were nonsmokers and 88.2% of men were smokers. Furthermore, smokers with more than 40 pack-years made up only 5.1% of all females and 58.6% of all males. That is, mean cigarette consumption was significantly lower in smoking women than in men. Such differences in smoking history likely resulted in different clinical presentation, histology, and treatment. It has been reported that the differences in smoking history may explain the better prognosis in females [8,30]. That is to say, gender is potential confounding factor in this study. In order to avoid systemic bias, we analyzed subgroup analyses.

In conclusion, the results of the current study found a preoperative smoking history to be a significant predictor of prognosis by univariate and multivariate analyses, in males. We showed a significant correlation between cigarette smoking and long-term disease-specific survival in stage IA NSCLC patients in numerous cases. The poor prognosis makes patients with smoking history an important population for creating stratification levels in clin-

ical trials and for the study of chemoprevention or smoking cessation study.

Acknowledgments

The authors are grateful to Dr. Keitaro Matsuo, Division of Epidemiology and Prevention, Aichi Cancer Center Research Institute, for his technical support in the statistical analysis and critical review. We also thank Drs. Shin Kawahara, Makoto Takeuchi, and Katsuyuki Kiura for their critical reviews.

The study was supported in part by a Grant-in-Aid for Cancer Research from the Ministry of Health, Labor, and Welfare, Japan.

References

[1] Pisani P, Parkin DM, Bray F, Ferlay J. Estimates of the worldwide mortality from 25 cancers in 1990. Int J Cancer 1999;83:18–29.

[2] Fry WA, Menck HR, Winchester DP. The National Cancer Data Base report on lung cancer. Cancer 1999;77:1947–55.

[3] Landis SH, Murray T, Bolden S, Wingo PA. Cancer statistics. CA Cancer J Clin 1999;49:8–31.

[4] Mountain CF. Revisions in the international system for staging lung cancer. Chest 1997;111:1710–7.

[5] Harpole Jr DH, Herndon Jr JE, Young Jr WG, Wolfe WG, Sabiston Jr DC. Stage I nonsmall cell lung cancer. A multivariate analysis of treatment methods and patterns of recurrence. Cancer 1995;76:787–96.

[6] Johnson BE. Second lung cancers in patients after treatment for an initial lung cancer. J Natl Cancer Inst 1998;90:1335–45.

[7] Harpole Jr DH, Herndon Jr JE, Wolfe WG, Iglehart JD, Marks JR. A prognostic model of recurrence and death in stage I non-small cell lung cancer utilizing presentation, histopathology, and oncoprotein expression. Cancer Res 1995;55:51–6.

[8] Hinds MW, Yang HY, Stemmermann G, Lee J, Kolonel LN. Smoking history and lung cancer survival in women. J Natl Cancer Inst 1982;68:395–9.

[9] Kato I, Tominaga S, Ikari A. Lung cancer prognostic factors from the Aichi Cancer Registry. Jpn J Clin Oncol 1990;20:238–45.

[10] Sobue T, Suzuki T, Fujimoto I, Doi O, Tateishi R, Sato T. Prognostic factors for surgically treated lung adenocarcinoma patients, with special reference to smoking habit. Jpn J Cancer Res 1991;82:33–9.

[11] Isobe T, Hiyama K, Yoshida Y, Fujiwara Y, Yamakido M. Prognostic significance of p53 and ras gene abnormalities in lung adenocarcinoma patients with stage I disease after curative resection. Jpn J Cancer Res 1994;85:1240–6.

[12] Suzuki K, Nagai K, Yoshida J, Nishimura M, Takahashi K, Yokose T, et al. Conventional clinicopathologic prognostic factors in surgically resected nonsmall cell lung carcinoma A comparison of prognostic factors for each pathologic TNM stage based on multivariate analyses. Cancer 1999;86:1976–84.

[13] Sioris T, Husgafvel-Pursiainen K, Karjalainen A, Anttila S, Kannio A, Salo JA, et al. Survival in operable non-small-cell lung cancer: role of p53 mutations, tobacco smoking and asbestos exposure. Int J Cancer 2000;86:590–4.

[14] Fujisawa T, Iizasa T, Saitoh Y, Sekine Y, Motohashi S, Yasukawa T, et al. Smoking before surgery predicts poor long-term survival in patients with stage I non-small-cell lung carcinomas. J Clin Oncol 1999;17:2086–91.

[15] Tammemagi MC, McLaughlin JR, Mullen JB, Bull SB, Johnston MR, Tsao MS, et al. A study of smoking, p53 tumor suppressor gene alterations and non-small cell lung cancer. Ann Epidemiol 2000;10:176–85.

[16] Lippman SM, Lee JJ, Karp DD, Vokes EE, Benner SE, Goodman GE, et al. Randomized phase III intergroup trial of isotretinoin to prevent second primary tumors in stage I non-small-cell lung cancer. J Natl Cancer Inst 2001;93:605–18.

[17] Linden G, Dunn Jr JE, Hom PH, Mann M. Effect of smoking on the survival of patients with lung cancer. Cancer 1972;30:325–8.

[18] Shimizu H, Tominaga S, Nishimura M, Urata A. Comparison of clinico-epidemiological features of lung cancer patients with and without a history of smoking. Jpn J Clin Oncol 1984;14:595–600.

[19] Ebina M, Steinberg SM, Mulshine JL, Linnoila RI. Relationship of p53 overexpression and up-regulation of proliferating cell nuclear antigen with the clinical course of non-small cell lung cancer. Cancer Res 1994;54:2496–503.

[20] Holli K, Visakorpi T, Hakama M. Smoking and survival from lung cancer. Acta Oncol 1999;38:989–92.

[21] Moores LK. Smoking and postoperative pulmonary complications. An evidence-based review of the recent literature. Clin Chest Med 2000;21:139–46.

[22] Ogle KS, Swanson GM, Woods N, Azzouz F. Cancer and comorbidity: redefining chronic diseases. Cancer 2000;88:653–63.

[23] Richardson GE, Tucker MA, Venzon DJ, Linnoila RI, Phelps R, Phares JC, et al. Smoking cessation after successful treatment of small-cell lung cancer is associated with fewer smoking-related second primary cancers. Ann Intern Med 1993;119:383–90.

[24] Kawahara M, Ushijima S, Kamimori T, Kodama N, Ogawara M, Matsui K, et al. Second primary tumours in more than 2-year disease-free survivors of small-cell lung cancer in Japan: the role of smoking cessation. Br J Cancer 1998;78:409–12.

[25] Kwiatkowski DJ, Harpole Jr DH, Godleski J, Herndon Jr JE, Shieh DB, Richards W, et al. Molecular pathologic substaging in 244 stage I non-small-cell lung cancer patients: clinical implications. J Clin Oncol 1998;16:2468–77.

[26] Taga S, Osaki T, Ohgami A, Imoto H, Yoshimatsu T, Yoshino I, et al. Prognostic value of the immunohistochemical detection of p16INK4 expression in nonsmall cell lung carcinoma. Cancer 1997;80:389–95.

[27] Niklinski J, Niklinska W, Laudanski J, Chyczewska E, Chyczewski L. Prognostic molecular markers in non-small cell lung cancer. Lung Cancer 2001;34(Suppl. 2):S53–8.

[28] Vahakangas KH, Bennett WP, Castren K, Welsh JA, Khan MA, Blomeke B, et al. p53 and K-ras mutations in lung cancers from former and never-smoking women. Cancer Res 2001;61:4350–6.

[29] Foucher P, Coudert B, Arveux P, Boutron MC, Kisterman JP, Bernard A, et al. Age and prognosis of non-small cell lung cancer. Usefulness of a relative survival model. Eur J Cancer 1993;29A:1809–13.

[30] Johnston-Early A, Cohen MH, Minna JD, Paxton LM, Fossieck Jr BE, Ihde DC, et al. Smoking abstinence and small cell lung cancer survival. An association. JAMA 1980;244:2175–9.

Role of Mitochondrial DNA in Cells Exposed to Irradiation: Generation of Reactive Oxygen Species (ROS) is Required for G2 Checkpoint upon Irradiation

Saori Kawamura,[a] Daisaku Takai,[a] Keiko Watanabe,[a] Jun-ichi Hayashi,[b] Kazushige Hayakawa,[c] and Makoto Akashi*,[a]

[a]*Department of Radiation Emergency Medicine, Research Center for Radiation Emergency Medicine, National Institute of Radiological Sciences, 4–9–1 Anagawa, Inage-ku, Chiba 263–8555, Japan,* [b]*Institute of Biological Sciences, University of Tsukuba, 1–1–1 Tennodai, Tsukuba, Ibaraki 305–8572, Japan, and* [c]*Department of Radiology, Kitasato University School of Medicine, 1–15–1 Kitasato, Sagamihara, Kanagawa 228–8555, Japan*

(Received February 4, 2005; Accepted February 7, 2005)

Mitochondria have their own genome encoding subunits of the electron transport chain. Using cells lacking mitochondrial DNA (mtDNA, ρ^0 cells), we studied the role of mtDNA in irradiation. Loss of mtDNA inhibited cell growth and reduced the level of reactive oxygen species (ROS) as compared to ρ^+ cells. ρ^+ cells were more resistant to irradiation than ρ^0 cells. Upon irradiation, ρ^0 cells showed delayed G2 arrest and decreased ability of a cell to recover from the G2 checkpoint compared to ρ^+ cells. Irradiation increased the generation of ROS even more in ρ^+ cells. Irradiation markedly increased the levels of phosphorylated forms of extracellular-regulated kinases, p42 and p44 (ERK1/2) in ρ^+ cells, whereas phosphorylated levels of the kinases were affected slightly in ρ^0 cells. Furthermore, inhibition of the ERK pathway led to a delayed G2 arrest and a delayed recovery from the arrest in irradiated ρ^+ cells, and treatment with NAC also induced dysfunction of the G2 checkpoint in irradiated ρ^+ cells. These results suggest that the accumulation of ROS potentiated ERK1/2 kinases after irradiation in ρ^+ cells, leading to less sensitivity to irradiation. Thus, mtDNA is important for the generation of ROS that act as second messenger.

Key words —— mitochondrial DNA, irradiation, reactive oxygen species, checkpoint

INTRODUCTION

Mitochondria have their own DNA (mtDNA) of 16 kilo base pairs in human cells. mtDNA encodes subunits of the mitochondrial electron transport chain. These subunits are essential for normal oxidative phosporylation and also adenosine triphosphate (ATP) production in a cell. Oxidative phosphorylation in mitochondria produces the large part of the energy required within a cell.[1] Human mtDNA has a mutational rate at least 10 times higher than nuclear DNA,[2] and somatic mutations in mtDNA have also been observed in human neoplasms.[3] Recently, there have been reports using cells lacking mtDNA that studied its roles in cell death or sensitivity to various external insults. Studies have shown that mtDNA-depleted cells are susceptible to cell death by serum-deprivation, tumor necrosis factor (TNF) and staurosporine.[4–6] On the other hand, studies found that these cells were more resistant to insults such as tumor necrosis factor-related apoptosis-inducing ligand (TRAIL), anti-cancer reagents, and reactive oxygen species (ROS) than their parental cells.[7,8] Thus, the roles of mtDNA are still not clear, and the mechanisms for the sensitivity to external insults remain unresolved.

The respiratory chain in mitochondria is a source of ROS.[9–12] On the other hand, studies have shown that ROS generated in mitochondria can modulate signaling cascades.[13–15] The pathway of the mitogen-activated protein kinase (MAPK) family is involved in growth factor-mediated regulation of diverse cellular events such as proliferation, senescence, differentiation and apoptosis.[16] Exposure of cells to oxidative stress such as irradiation induces activation of multiple MAPK pathways; these signals play critical roles in controlling cell survival and repopulation effects following irradiation.[16] The MAPK superfamily is composed of several signal-

*To whom correspondence should be addressed: Department of Radiation Emergency Medicine, Research Center for Radiation Emergency Medicine, National Institute of Radiological Sciences, 4–9–1 Anagawa, Inage-ku, Chiba 263–8555 Japan. Tel.: +81-43-206-3122; Fax: +81-43-284-1736; E-mail: akashi@nirs.go.jp

ing pathways: mitogen-activated extracellular-regulated kinases, p42 and p44 (ERK1/2), c-Jun N-terminal kinase (JNK), and p38 pathways. ERK1/2 are serine/threonine kinases that are regulated by mitogen-activated/extracellular-regulated kinase 1/2 (MEK1/2) through phosphorylation. The activation of ERK1/2 protects cells against noxious stimuli in several ways and inhibits apoptosis through the activation of caspase or the inhibition of cytochrome c release.[17,18] Furthermore, ERK1/2 activation has been reported to promote several transcriptional factors such as nuclear factor-kappa B (NF-κB) and cyclic adenosine monophosphate responsive element binding protein (CREB), which then stimulate the expression of anti-apoptotic genes.[19] The activation of ERK1/2 has been reported to abrogate the G2/M phase arrest after irradiation in some cell types.[20,21] In contrast, JNK and p38 MAPK have been reported to mediate caspase activation, resulting in apoptosis.[16] However, the roles of mtDNA and how ROS generated in mitochondria affect signaling pathways are not fully understood in cells exposed to irradiation.

The recent progress in studies of mitochondria has allowed us to use mtDNA-depleted cells (ρ^0cells) and their control cells (ρ^+ cells). Elimination of mtDNA from cells can be performed by long-term exposure to a low concentration of 3,8-diamino-5-ethyl-6-phenylphenanthridinium bromide (ethidium bromide; EtBr).[22] ρ^+ cells are produced by the fusion of cytoplasts from the parent cells with ρ^0 cells, and these cells possess normal mtDNA. By comparing ρ^0 to ρ^+ cells, the roles of mtDNA can be determined. Irradiation is well known to induce apoptosis and cause DNA damage. However, there are few studies on the roles of mtDNA in irradiated cells. In the present study, we investigated the roles of mtDNA in irradiated cells by comparing ρ^0 cells lacking mtDNA and their control ρ^+ cells. We found that ρ^0 cells were more radiosensitive than ρ^+ cells, and demonstrated that homeostatic mitochondrial ROS production may have a protective effect on cells exposed to irradiation through MEK activation and cell cycle control.

MATERIAL AND METHODS

Cells and Cell Culture —— Cells used in this study originated from HeLa cells: ρ^0 cells (EB8-C) lacking mtDNA, and ρ^+ cells (HeEB5) cybrid clones produced by fusion of EB8-C cells and cytoplasts of HeLa cells.[22,23] For cell culture, the medium consisted of RPMI 1640 (Gibco, Invitrogen Corp., CA, U.S.A.) supplemented with 10% (v/v) fetal bovine serum (INTERGEN, Purchase, NY, U.S.A.), 50 μg/ml of uridine (Sigma, St. Louis, MO, U.S.A.) and 1 mM of sodium pyruvate (Gibco).

Polymerase Chain Reaction (PCR) —— Total DNA was extracted by the phenol/chloroform method. Primers were specific for the segment of mitochondrial DNA: forward, 5′-atg ccc caa cta aat act acc g-3′ and reverse, 5′-gtg gtg att agt cgg ttg ttg a-3′. After electrophoresis on 2% agarose, the 298-bp fragment was analyzed with ethidium bromide (Sigma) under UV light.

Clonogenic Assays —— For colony formation assay, 10^2 to 5×10^3 cells were seeded in 60-mm culture plates 18 hr before irradiation at various doses. Colonies were stained and counted after 14 days; groups of cells containing at least 50 cells were defined as a colony. Colonies with diameter greater than 1.2 mm were defined as "larger colonies" using Intelligent Quantifier™ (Bio Image Systems, Inc., Jackson, MI, U.S.A.). Survival curves are representative data from three independent experiments.

Radiation Setting —— ^{137}Cs source emitting at a fixed dose rate of 10 Gy/min was used for γ-ray irradiation.

Cell Cycle Analysis —— After irradiation, cells were fixed with 70% ethanol at the times indicated. Then the cells were incubated for 30 min at 37°C with 1 μg/ml RNase A, stained with 50 μg/ml propidium iodide and filtered through nylon mesh with a pore size of 50–70 μm. Cell cycle profiles were evaluated by FACScaliber flow cytometry (Becton Dickinson, Bedford, MA, U.S.A.).

Analysis of Intracellular ROS Production —— 2′,7′-dichlorofluorescein (DCF) is one of the most prevalent oxidant-sensitive fluorescent dye. Acetyl ester derivative of dihydro-DCF diacetate (CM-H_2DCFDA, Molecular Probes, Eugene, OR, U.S.A.), a derivative of DCF, was used in this study. Cells were prepared 18 hr before the treatment to a cell count of 6×10^5 for each 60-mm diameter dish. After irradiation, cells were stained with 10 μM CM-H_2DCFDA at 37°C for 5 min. Fluorescence intensity was measured by flow cytometry with excitation at 488 nm and emission at 530 nm.

Western-Blot Analysis —— The cells were lysed in buffer containing 50 mM Tris–HCl (pH 8.0), 150 mM NaCl, 3 mM NaN_3, 0.1% (w/v) sodium dodecyl sulfate (SDS), 1% (v/v) Nonidet P-40 and 0.5% sodium deoxycholate. The protein concentra-

tion of each sample was measured by the method of Bradford (Bio-Rad, Hercules, CA, U.S.A.).[24] Electrophoresis was performed with samples containing 50 μg of cell lysates in SDS-polyacrylamide gel electrophoresis (PAGE) loading buffer using 10% polyacrilamide gel, followed by transfer of the proteins onto pure nitrocellulose membranes (Trans-Blot Transfer Membrane; Bio-Rad). Immunoreactivity was detected by enhanced chemiluminescence (Amersham Biosciences). The relative density of bands was determined by Intelligent Quantifier program (Bio Image, Ann Arbor, MI, U.S.A.) and normalized to the loading control.

RESULTS

ρ^0 Cells Lacking mtDNA

ρ^0 cells lacking mtDNA (named HeLa EB8-C) were made by long-term EtBr treatment.[23] ρ^+ cells (HeEB5) were cybrids of EB8-C cells with intact mtDNA. To confirm the absence of mtDNA, the 298-bp segment of mtDNA was amplified by polymerase chain reaction (PCR) analysis (Fig. 1). No detectable band corresponding to mtDNA was noted in EB8-C cells, whereas clear bands were amplified in HeEB5 cells. We also confirmed the absence of mtDNA by the failure to grow in the absence of uridine in the medium, since ρ^0 cells are dependent on uridine and pyruvate for growth because of the absence of a functional respiratory chain[22] (data not shown). Thus, EB8-C cells were proven to be defective in oxidative phosphorylation and were used in the present study.

Lower Production of ROS in EB8-C Cells

CM-H_2DCFDA was used for experiments because of its better retention within cells than DCF. We compared ROS generation in HeEB5 and EB8-C cells by flow cytometry. The mean fluorescence intensities of untreated HeEB5 and EB8-C cells were 51 ± 4 and 26 ± 2, respectively, indicating that HeEB5 cells produced ROS constitutively at a higher level than EB8-C cells ($p < 0.005$).

The ROS production is known to increase after irradiation in cells.[12,25] The generation of ROS was evaluated at 30 min after irradiation in the two cell lines. Exposure to irradiation with 20 Gy resulted in significantly increased fluorescence intensity in HeEB5 cells (136 ± 10, 2.6-fold, $p < 0.01$), but the fluorescent intensities were not increased in EB8-C cells (23 ± 1).

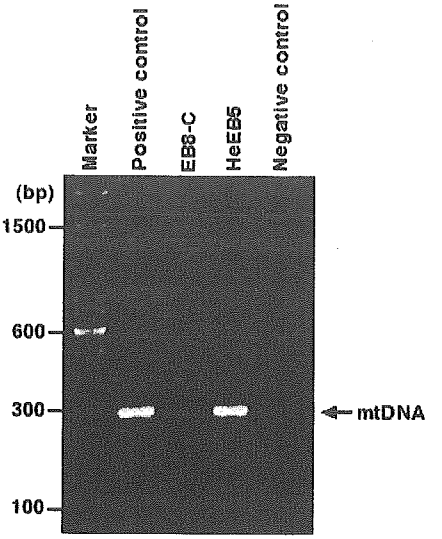

Fig. 1. Comparison between EB8-C and HeEB5 Cells
mtDNA was amplified by PCR as described in MATERIALS AND METHODS. The arrow indicates 298-bp fragments of mtDNA. SK-HEP-1 hepatocellular carcinoma cells were used as positive control. As negative control, purified water was used.

The specificity of ROS was also determined by irradiation in the presence of catalase from human erythrocytes (Calbiochem, La Jolla, CA, U.S.A.) in HeEB5 cells. The treatment with catalase abolished the irradiation-induced increase in the fluorescent intensity (data not shown). Furthermore, irradiated HeEB5 cells were stained with dihydroethidium (DHE, Molecular Probes) specific for superoxide radicals. However, an increased intensity of fluorescence was not detected in these cells (data not shown). These results suggest that irradiation increased the level of ROS, mainly hydrogen peroxide in HeEB5 cells.

Increased Sensitivity of EB8-C Cells to Irradiation

Next we sought to determine whether the observed difference in ROS production affects the survival and growth of cells after irradiation. Cellular radiosensitivity was analyzed by colony formation assay. The plating efficiencies were 87.7 ± 2.5 and 50.3 ± 4.5% in HeEB5 cells and EB8-C cells, respectively, and the efficiency was significantly reduced in EB8-C cells ($p < 0.001$). Further study found a significantly reduced survival fraction in EB8-C irradiated with 2 Gy (Fig. 2). The surviving fractions were 0.33 ± 0.01 and 0.19 ± 0.03 in HeEB cells and EB8-C cells, respectively ($p < 0.01$). At 4 Gy of irradiation, the fractions were 0.21 ± 0.02 for HeEB5 cells and 0.06 ± 0.00 for EB8-C cells,

showing a significantly decreased survival fraction in EB8-C cells compared to HeEB5 cells ($p < 0.005$). Upon irradiation with either 6 or 8 Gy, significant differences in sensitivity to irradiation were observed between these cell lines.

To further evaluate the cell growth after irradiation, the diameter of the colonies was quantitatively evaluated (Table 1). HeEB5 cells had a significantly higher capacity for forming colonies larger than 1.2 mm in diameter than EB8-C cells. The capacity for forming larger colonies was 15.1 ± 1.7% in the control. On the other hand, 5.5 ± 0.2% of untreated EB8-C cells formed larger colonies. HeEB5 cells also formed larger colonies than EB8-C cells at each dose of irradiation. At 1 Gy, HeEB5 cells had 14.7 ± 3.1% of the capacity, whereas that of EB8-C cells was 1.8 ± 0.4%. Thus, depleting mtDNA affected cell growth and resulted in an increased sensitivity to irradiation.

Dysfunction of the G2 Checkpoint in Irradiated EB8-C Cells

Cells have mechanisms to delay or halt cell cycle progression in response to genotoxic insult to maintain genomic integrity.[26] HeLa cells are known to be infected with human papilloma virus, of which the E6 protein inactivates p53; the checkpoint may not function in cells exposed to ionizing radiation.[27] To determine whether such checkpoint mechanisms are associated with the observed sensitivity to irradiation in EB8-C cells, cell cycle progression after irradiation was studied (Table 2). Without irradiation, the cell cycle profiles of both cell lines were similar. After irradiation with 8 Gy, 60% of HeEB5 cells had entered the G2 phase by 12 hr. Thereafter, the cells gradually re-entered G1 and then S phase by 36 hr. On the other hand, the cell cycle progression was delayed after irradiation in EB8-C cells when compared to HeEB5 cells. Cells gradually entered the G2 phase by 24 hr, and 60% of cells remained at G2 phase 36 hr after irradiation. Thus, EB8-C cells showed delayed induction of G2 arrest and decreased ability to recover from G2 arrest.

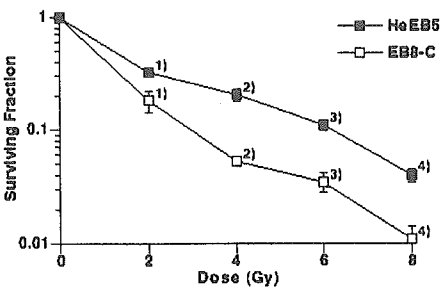

Fig. 2. Radiosensitivity of Cells Lacking mtDNA

HeEB5 and EB8-C cells were exposed to ionizing radiation at indicated doses. After two weeks, colonies were stained with hematoxilin-eosin and counted. All experiments were triplicated. The results were the mean of three independent experiments. 1) $p < 0.01$, 2–4) $p < 0.005$.

Activation of ERK Pathway in Irradiated HeEB5 Cells

Previously, we have shown that MAPK is involved in the sensitivity to irradiation.[28] To study the mechanism causing the different sensitivity to irradiation in the two cell lines, the MAPK pathway was determined. Cells were irradiated at a dose of 8 Gy and cultured for 1 hr. Western blot analysis using antibody recognizing the phosphorylated form of ERK1/2 showed that it was more abundant in untreated HeEB5 cells than in untreated EB8-C cells; EB8-C cells had a faint band of phosphorylated form of ERK1/2 (Fig. 3). HeEB5 cells had almost 4-fold higher level of phosphorylated form of ERK1/2 as compared to that of EB8-C cells. Irradiation activated ERK1/2 by 2-fold in HeEB5 cells. However, irradiation failed to increase the level of phosphorylated form of ERK1/2 in EB8-C cells. Thus, the activation of the ERK pathway was much more prominent in HeEB5 cells than in EB8-C cells. We also studied the effect of irradiation on the phosphorylation of p38MAPK in these cells. However, phosphorylation of p38MAPK was not induced in both cell lines (data not shown).

Table 1. Numbers of Colonies Larger than 1.2 mm after Irradiation in HeEB5 and EB8-C Cells

	Percentage of larger colonies					
	0	1	2	4	6	8 (Gy)
HeEB5	15.1 ± 1.7[a)]	14.7 ± 3.1[b)]	11.9 ± 1.1[c)]	8.2 ± 1.2[d)]	6.4 ± 0.5[e)]	5.8 ± 0.9[f)]
EB8-C	5.5 ± 0.2[a)]	1.8 ± 0.4[b)]	1.4 ± 0.4[c)]	1.1 ± 0.0[d)]	0.2 ± 0.1[e)]	2.0 ± 0.2[f)]

Cells were irradiated at indicated doses and the numbers of colonies (> 1.2 mm in diameter) were calculated as described in "MATERIALS AND METHODS." All experiments were triplicated and representative results of three independent experiments are shown as mean ± S.D. *a)* $p < 0.01$, *b,d,f)* $p < 0.05$, *c,e)* $p < 0.005$.

Table 2. Cell Cycle Profile after Irradiation in HeEB5 and EB8-C Cells

		Distribution of Cells in Each Stage (%)				
	Stage	0 hr	8 hr	12 hr	24 hr	36 hr
HeEB5						
Untreated	G_1	46	51	52	54	54
	S	35	30	32	30	31
	G_2/M	19	19	16	16	15
IR (8 Gy)	G_1		19	6	48	42
	S		46	34	9	36
	G_2/M		35	60	42	22
EB8-C						
Untreated	G_1	55	57	55	55	59
	S	31	38	30	31	30
	G_2/M	14	15	15	14	11
IR (8 Gy)	G_1		31	19	3	35
	S		50	49	9	5
	G_2/M		19	32	88	60

HeEB5 and EB8-C cells were irradiated at a dose of 8 Gy and harvested at the times indicated. Cells were fixed with 70% ethanol and treated with RNase A. Then, cells were stained with propidium iodide (PI) and the DNA content was analyzed by flow cytometry using CellQuest and Modifit programs.

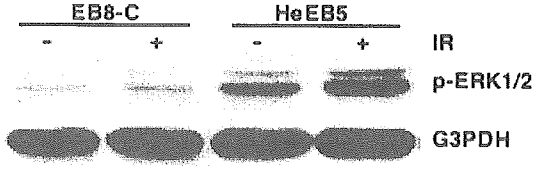

Fig. 3. Expression of ERK in Cells Exposed to Ionizing Radiation

Cells were incubated for an hour after irradiation with 8 Gy. Whole cell lysates were used for immunoblotting with anti-phosphorylated ERK1/2 antibody (Thr202/Tyr204, Cell Signaling Technology, Inc. Beverly, MA, U.S.A.). As loading control, glyceroaldehyde-3-phosphate dehydrogenase (G3PDH) was used. The results are representative of three independent experiments.

Inhibition of ERK Pathway Results in Dysfunctional G2 Checkpoint in Irradiated Cells

MEK2 activation has been reported to be essential for cellular recovery from the G2 phase arrest and subsequent survival in irradiated HeLa cells.[20] To study whether the ERK pathway is involved in the cell cycle delay of irradiated cells, cells were pretreated with MEK1/2 inhibitors, either PD98059 (50 μM) or U0126 (10 μM), for 1 hr and then irradiated at 8 Gy in the presence of these inhibitors. Twenty-four hours after irradiation, the cell cycle distribution of the cells was analyzed (Table 3). HeEB5 cells cycled more rapidly after irradiation than EB8-C cells; 62% of cells had re-entered the G1 phase by 24 hr, whereas 83% of EB8-C cells remained at the G2 phase (see also Table 2). On the other hand, treatment with either PD98059 or U0126 induced delayed recovery from the G2 checkpoint in irradiated HeEB5 cells; 46 and 57% of cells treated with PD98059 and U0126 stayed at the G2 phase 24 hr after irradiation, respectively. In contrast, treatment with either of these inhibitors did not affect the cell cycle profile in irradiated EB8-C cells.

To further determine whether ROS generated in cells exposed to irradiation affect cell cycle progression, these cells were treated with 25 mM of a free radical scavenger N-acetyl cystein (NAC) for 1 hr, and then irradiated at 8 Gy in the presence of NAC. The cell cycle was analyzed 24 hr after irradiation. NAC treatment also resulted in the delayed recovery from irradiation-induced G2 arrest in HeEB5 cells; 62% of the cells were at G2/M phase. However, NAC accelerated the recovery slightly in irradiated EB8-C cells. In parallel, the numbers of colonies were counted 2 weeks later. A significantly decreased sensitivity was observed in EB8-C cells; the surviving fractions were $3.3 \pm 0.8\%$ for HeEB5 cells and $1.6 \pm 0.5\%$ for EB8-C cells, respectively ($p < 0.05$). Treatment with NAC reduced the surviving fraction in irradiated HeEB5 cells ($0.7 \pm 0.2\%$, $p < 0.05$). In contrast, pretreatment with the compound had no significant effect on the fraction of irradiated EB8-C cells ($0.6 \pm 0.5\%$).

Table 3. Effect of MEK1/2 Inhibition and ROS Scavenger on Cell Cycle Progression after Irradiation

		Distribution of Cells in Each Stage (%)				
		Untreated	IR	PD+IR	U+IR	NAC+IR
HeEB5	G_1	55	62	46	37	32
	S	30	15	8	6	6
	G_2/M	15	23	46	57	62
EB8-C	G_1	56	7	4	7	9
	S	31	10	14	12	22
	G_2/M	13	83	82	81	69

Cells were pretreated with either MEK inhibitor PD98059 (PD, 50 μM, Calbiochem, La Jolla, CA, U.S.A.), U0126 (U, 10 μM, Cell Signaling Technology, Inc., Beverly, MA, U.S.A.) or a free radical scavenger N-acetyl cysteine (NAC, 25 mM, Sigma) for 1 hr. Then cells were irradiated with 8 Gy. Twenty-four hr after irradiation, cell cycle analysis with propidium iodide staining was performed. Data are representative of three independent experiments.

DISCUSSION

ROS are ubiquitously generated at a steady state, and their production is enhanced by irradiation.[29] mtDNA is more vulnerable to oxidative stress than nuclear DNA.[2] Furthermore, mtDNA is continuously replicated even in terminally differentiated cells. It is therefore of major importance that the role(s) of mtDNA in irradiated cells is clarified. In the present study, we compared cells without mtDNA (ρ^0 cells, EB8-C) to control cells with intact mtDNA (ρ^+ cells, HeEB5) in irradiation. EB8-C cells produced less amounts of ROS than HeEB5 cells both at a steady state and following irradiation. We also showed that EB8-C cells were more sensitive to irradiation than HeEB5 cells, a phenomenon associated with lower post-irradiation ROS production. Irradiated HeEB5 cells exhibited earlier recovery from irradiation-induced G2 arrest, which was blocked by either MEK inhibition or scavenging ROS.

Induction of cell cycle checkpoint responses in cells exposed to irradiation is essential for maintaining genomic integrity by the repair of damaged DNA.[26] Oxidative stress such as irradiation causes G1 arrest that is dependent on p53 activation.[26] Since effective G2 arrest and recovery from G2 arrest have also been shown to be essential for the ability of the cell to respond effectively to irradiation, we analyzed the cell cycle profile of HeEB5 and EB8-C cells after irradiation. Following irradiation, HeEB5 cells did not arrest in the G1 phase, entering into the G2 phase. These results were consistent with a previous study reporting that the G2 checkpoint showed arrest due to irradiation damage in HeLa cells.[30] On the other hand, the cell cycle progression of irradiated EB8-C cells was delayed, as these cells induced delayed G2 arrest. In addition, HeEB5 cells exited faster from the G2 phase than EB8-C cells, with the latter demonstrating a delayed recovery from the G2 arrest. Previous studies showed that reconstitution of p53-null cells with functional p53 shortened G2 arrest upon irradiation,[31] and that bone marrow cells enriched in normal myeloblasts entered mitosis more frequently than p53-null cells after exposure to irradiation.[32,33] Moreover, in ataxia telangiectasia (AT) cells, the DNA damage-dependent G2 arrest is longer than in normal cells,[34] and the length of G2 arrest has been reported to correlate with the radioresistance of the cell.[33] These studies suggest that the prolonged G2 phase following DNA damage is due to lower repair efficiency. However, mtDNA does not code for any DNA repair protein. Therefore, our results suggest that activation of mtDNA might lead to initiating a certain signal transduction pathway that protects cells from irradiation. HeEB5 and EB8-C cells originate from HeLa cells.[23] HeLa cells are infected with human papilloma virus and the E6 protein inactivates p53.[27] $p21^{WAF1}$ is one of the cyclin dependent kinase (Cdk) inhibitors regulated by p53 and causes cell cycle arrest.[35] However, $p21^{WAF1}$ is also induced by p53-independednt mechanisms following irradiation.[36] Therefore, we studied the expression of $p21^{WAF1}$ in these cells. The $p21^{WAF1}$ expression was not induced by irradiation in HeEB5 and EB8-C cells (data not shown). Our results thus suggest that the increased sensitivity to irradiation and the delayed G2 arrest and delayed recovery from G2 arrest constitute a p53-independent event in these cells.

The MAPK pathways control cell fate in irradiated cells, and ERK signaling is important for radiation sensitivity.[16] ROS and irradiation are also known to activate MAPK pathways.[6,37,38] Moreover,

MAPK pathways are necessary for cell cycle progression through G2.[39] We studied phosphorylation of ERK1/2 in both cell lines irradiated. The phosphorylated form of ERK1/2 was clearly detected in HeEB5 cells and irradiation activated ERK1/2 in these cells. However, irradiation did not activate p38MAPK in both cells (not shown). Moreover, treatment with two different inhibitors specific for MEK1/2 delayed the recovery from G2 arrest in irradiated HeEB5 cells. Interestingly, scavenging ROS with NAC clearly induced the delayed recovery and also increased the radiation sensitivity in these cells. In EB8-C cells, however, irradiation only slightly activated the phosphorylation of ERK1/2, and NAC also induced delayed G2 arrest, albeit only to a minor extent. However, treatment with these inhibitors did not affect the cell cycle following irradiation in EB8-C cells. Thus, our study showed that the generation of ROS is involved in the regulation of the G2 checkpoint and that mtDNA is important for increased ROS generation leading to the potentiation of the ERK1/2 pathway to a certain extent in irradiated cells. It has been reported that inhibition of MEK2 upstream of ERK1/2 increased radiosensitivity through a deregulated G2 checkpoint and that treatment with caffeine reversed the radiosensitivity with a concomitant recovery from the G2 arrest in otherwise terminally arrested HeLa cells with MEK2 mutation.[20] In A431 squamous carcinoma cells and DU 145 prostate carcinoma cells, inhibition of MEK1/2 by PD 98059 slowed recovery from the G2/M arrest and enhanced cell death.[21,40] Taken together, our results indicate that the efficient activation of the ERK1/2 pathway by the generation of ROS is required for protection of cells from irradiation through the recovery from irradiation-induced G2 arrest in cells. However, mtDNA-depleted cells are unable to activate the ERK pathway because of their disability to effectively generate ROS, whereas NAPDH oxidase existing in cellular membrane and epidermal growth factor-induced production may be source of ROS outside mitochondria[10] and ROS production related to cytochrome c may be also source.[41] Thus, it is clear that mtDNA is important for signal transduction as well as oxidative phosphorylation.

mtDNA is a circular, double-stranded molecule encoding 13 proteins that compose part of complex I, III–V (ATP synthase) of the electron transport chain.[42] Mammalian mitochondria account for over 90% of cellular oxygen consumption, and 1–5% of consumed oxygen is converted to ROS in the mitochondrial respiratory chain.[43] We compared the production of ROS between EB8-C and HeEB5 cells, since the mitochondrial respiratory chain is a powerful source of ROS. HeEB5 cells had a constitutively higher level of ROS with lower activity of glutathione peroxidase (GSH-Px) than EB8-C cells (data not shown). Previous studies by other investigators have also reported decreased generation of ROS in cells lacking mtDNA.[9,10,12] We also found greater plating efficiency and larger sizes of colonies in HeEB5 cells than in EB8-C cells. These results indicate that HeEB5 cells have higher growth rate. Our results also suggest that steady-state levels of ROS produced in a regulated fashion may be required for signaling pathways controlling essential cellular function, whereas high levels of ROS may inhibit the activity of cellular components or result in damage and cell death. Thus, mtDNA may play an important role in the generation of ROS that initiate the signal transduction for cell growth.

We studied the role of mtDNA in irradiated cells and showed that EB8-C cells were more sensitive to irradiation. These results are in contrast to those of studies by other investigators, who reported that ρ^0 cells are resistant to various forms of stress such as oxidative stress, chemicals, TRAIL, and others.[6–8,44] The mechanisms responsible for these discrepancies are not clear. One of these studies concluded that up-regulation of manganese superoxide dismutase (MnSOD) and GSH-Px leads to an efficient disposal of increased oxidative stress and increased resistance against ROS in ρ^0 cells.[7] In our study, on the other hand, the activity of MnSOD was higher with no difference in that of copper-zinc superoxide dismutase (CuZnSOD) but the activity of GSH-Px was lower in HeEB5 cells, and no difference of catalase (CAT) levels were observed in both cell lines (data not shown). Increased activities of SODs lead to the accumulation of H_2O_2 unless the H_2O_2 is in turn detoxified by GSH-Px or catalase. Furthermore, our study showed that scavenging ROS with NAC significantly reduced the colony forming capacity in irradiated HeEB5 cells, whereas NAC did not affect that in irradiated EB8-C cells. We could not detect an increase of the ROS generation in cells irradiated with 8 Gy or less in our experiments. However, NAC treatment delayed the recovery from G2 in irradiated HeEB5 cells with 8 Gy and also increased the radiation sensitivity of HeEB5 cells. Our results strongly suggest that mtDNA plays an important role in initiating a certain signal transduction pathway leading to cell survival, whereas the

role of ROS may vary according to cell type and their concentrations produced.

Acknowledgements This work is supported in part by a Grant-in-Aid for Science Research from the Japan Society for the Promotion of Science (JSPS) (No. 16591242) and also a research project of the Radiation Emergency Medical Preparedness by National Institute of Radiological Sciences. We would like to thank Ms. Aki Yamamoto and Ms. Kyoko Takayama for their secretarial assistance.

REFFERENCES

1) Saraste, M. (1999) Oxidative phosphorylation at the fin de siecle. *Science*, **283**, 1488–1493.
2) Brown, W. M., George, M., Jr. and Wilson, A. C. (1979) Rapid evolution of animal mitochondrial DNA. *Proc. Natl. Acad. Sci. U.S.A.*, **76**, 1967–1971.
3) Tan, D. J., Bai, R. K. and Wong, L. J. (2002) Comprehensive scanning of somatic mitochondrial DNA mutations in breast cancer. *Cancer Res.*, **62**, 972–976.
4) Escary, J. L., Perreau, J., Dumenil, D., Ezine, S. and Brulet, P. (1993) Leukaemia inhibitory factor is necessary for maintenance of haematopoietic stem cells and thymocyte stimulation. *Nature* (London), **363**, 361–364.
5) Marchetti, P., Susin, S. A., Decaudin, D., Gamen, S., Castedo, M., Hirsch, T., Zamzami, N., Naval, J., Senik, A. and Kroemer, G. (1996) Apoptosis-associated derangement of mitochondrial function in cells lacking mitochondrial DNA. *Cancer Res.*, **56**, 2033–2038.
6) Jiang, S., Cai, J., Wallace, D. C. and Jones, D. P. (1999) Cytochrome c-mediated apoptosis in cells lacking mitochondrial DNA. Signaling pathway involving release and caspase 3 activation is conserved. *J. Biol. Chem.*, **274**, 29905–29911.
7) Park, S. Y., Chang, I., Kim, J. Y., Kang, S. W., Park, S. H., Singh, K. and Lee, M. S. (2004) Resistance of mitochondrial DNA-depleted cells against cell death: role of mitochondrial superoxide dismutase. *J. Biol. Chem.*, **279**, 7512–7520.
8) Kim, J. Y., Kim, Y. H., Chang, I., Kim, S., Pak, Y. K., Oh, B. H., Yagita, H., Jung, Y. K., Oh, Y. J. and Lee, M. S. (2002) Resistance of mitochondrial DNA-deficient cells to TRAIL: role of Bax in TRAIL-induced apoptosis. *Oncogene*, **21**, 3139–3148.
9) Li, N., Ragheb, K., Lawler, G., Sturgis, J., Rajwa, B., Melendez, J. A. and Robinson, J. P. (2003) Mitochondrial complex I inhibitor rotenone induces apoptosis through enhancing mitochondrial reactive oxygen species production. *J. Biol. Chem.*, **278**, 8516–8525.
10) Walford, G. A., Moussignac, R. L., Scribner, A. W., Loscalzo, J. and Leopold, J. A. (2003) Hypoxia potentiates nitric oxide-mediated apoptosis in Endothelial cells via peroxynitrite-induced activation of mitochondria-dependent and -independent pathways. *J. Biol. Chem.*, **279**, 4425–4432.
11) Sidoti-de Fraisse, C., Rincheval, V., Risler, Y., Mignotte, B. and Vayssiere, J. L. (1998) TNF-alpha activates at least two apoptotic signaling cascades. *Oncogene*, **17**, 1639–1651.
12) Leach, J. K., Van Tuyle, G., Lin, P. S., Schmidt-Ullrich, R. and Mikkelsen, R. B. (2001) Ionizing radiation-induced, mitochondria-dependent generation of reactive oxygen/nitrogen. *Cancer Res.*, **61**, 3894–3901.
13) Nemoto, S., Takeda, K., Yu, Z. X., Ferrans, V. J. and Finkel, T. (2000) Role for mitochondrial oxidants as regulators of cellular metabolism. *Mol. Cell. Biol.*, **20**, 7311–7318.
14) Waypa, G. B., Chandel, N. S. and Schumacker, P. T. (2001) Model for hypoxic pulmonary vasoconstriction involving mitochondrial oxygen sensing. *Circ. Res.*, **88**, 1259–1266.
15) Nishikawa, T., Edelstein, D., Du, X. L., Yamagishi, S., Matsumura, T., Kaneda, Y., Yorek, M. A., Beebe, D., Oates, P. J., Hammes, H. P., Giardino, I. and Brownlee, M. (2000) Normalizing mitochondrial superoxide production blocks three pathways of hyperglycaemic damage. *Nature* (London), **404**, 787–790.
16) Dent, P., Yacoub, A., Fisher, P. B., Hagan, M. P. and Grant, S. (2003) MAPK pathways in radiation responses. *Oncogene*, **22**, 5885–5896.
17) Shonai, T., Adachi, M., Sakata, K., Takekawa, M., Endo, T., Imai, K. and Hareyama, M. (2002) MEK/ERK pathway protects ionizing radiation-induced loss of mitochondrial membrane potential and cell death in lymphocytic leukemia cells. *Cell Death Differ.*, **9**, 963–971.
18) Tran, S. E., Holmstrom, T. H., Ahonen, M., Kahari, V. M. and Eriksson, J. E. (2001) MAPK/ERK overrides the apoptotic signaling from Fas, TNF, and TRAIL receptors. *J. Biol. Chem.*, **276**, 16484–16490.
19) Yang, S. H., Sharrocks, A. D. and Whitmarsh, A. J. (2003) Transcriptional regulation by the MAP kinase signaling cascades. *Gene*, **320**, 3–21.
20) Abbott, D. W. and Holt, J. T. (1999) Mitogen-activated protein kinase kinase 2 activation is essential for progression through the G2/M checkpoint arrest in cells exposed to ionizing radiation. *J. Biol. Chem.*, **274**, 2732–2742.

21) Hagan, M., Wang, L., Hanley, J. R., Park, J. S. and Dent, P. (2000) Ionizing radiation-induced mitogen-activated protein (MAP) kinase activation in DU145 prostate carcinoma cells: MAP kinase inhibition enhances radiation-induced cell killing and G2/M-phase arrest. *Radiat. Res.*, **153**, 371–383.
22) King, M. P. and Attardi, G. (1989) Human cells lacking mtDNA: repopulation with exogenous mitochondria by complementation. *Science*, **246**, 500–503.
23) Hayashi, J., Ohta, S., Kikuchi, A., Takemitsu, M., Goto, Y. and Nonaka, I. (1991) Introduction of disease-related mitochondrial DNA deletions into HeLa cells lacking mitochondrial DNA results in mitochondrial dysfunction. *Proc. Natl. Acad. Sci. U.S.A.*, **88**, 10614–10618.
24) Bradford, M. M. (1976) A rapid and sensitive method for the quantitation of microgram quantities of protein utilizing the principle of protein-dye binding. *Anal. Biochem.*, **72**, 248–254.
25) Morales, A., Miranda, M., Sanchez-Reyes, A., Biete, A. and Fernandez-Checa, J. C. (1998) Oxidative damage of mitochondrial and nuclear DNA induced by ionizing radiation in human hepatoblastoma cells. *Int. J. Radiat. Oncol. Biol. Phys.*, **42**, 191–203.
26) Shackelford, R. E., Kaufmann, W. K. and Paules, R. S. (2000) Oxidative stress and cell cycle checkpoint function. *Free Radic. Biol. Med.*, **28**, 1387–1404.
27) Werness, B. A., Levine, A. J. and Howley, P. M. (1990) Association of human papillomavirus types 16 and 18 E6 proteins with p53. *Science*, **248**, 76–79.
28) Takada, Y., Hachiya, M., Park, S. H., Osawa, Y., Ozawa, T. and Akashi, M. (2002) Role of reactive oxygen species in cells overexpressing manganese superoxide dismutase: mechanism for induction of radioresistance. *Mol. Cancer Res.*, **1**, 137–146.
29) Yang, Y. and Yu, X. (2003) Regulation of apoptosis: the ubiquitous way. *FASEB J.*, **17**, 790–799.
30) Maity, A., Kao, G. D., Muschel, R. J. and McKenna, W. G. (1997) Potential molecular targets for manipulating the radiation response. *Int. J. Radiat. Oncol. Biol. Phys.*, **37**, 639–653.
31) Schwartz, D., Almog, N., Peled, A., Goldfinger, N. and Rotter, V. (1997) Role of wild type p53 in the G2 phase: regulation of the gamma-irradiation-induced delay and DNA repair. *Oncogene*, **15**, 2597–2607.
32) Lavin, M. F. and Shiloh, Y. (1997) The genetic defect in ataxia-telangiectasia. *Annu. Rev. Immunol.*, **15**, 177–202.
33) Aldridge, D. R. and Radford, I. R. (1998) Explaining differences in sensitivity to killing by ionizing radiation between human lymphoid cell lines. *Cancer Res.*, **58**, 2817–2824.
34) Hawley, R. S. and Friend, S. H. (1996) Strange bedfellows in even stranger places: the role of ATM in meiotic cells, lymphocytes, tumors, and its functional links to p53. *Genes Dev.*, **10**, 2383–2388.
35) Gartel, A. L. and Tyner, A. L. (2002) The role of the cyclin-dependent kinase inhibitor p21 in apoptosis. *Mol. Cancer Ther.*, **1**, 639–649.
36) Akashi, M., Hachiya, M., Osawa, Y., Spirin, K., Suzuki, G. and Koeffler, H. P. (1995) Irradiation induces WAF1 expression through a p53-independent pathway in KG-1 cells. *J. Biol. Chem.*, **270**, 19181–19187.
37) Torres, M. (2003) Mitogen-activated protein kinase pathways in redox signaling. *Front Biosci.*, **8**, 369–391.
38) Zhang, Z., Leonard, S. S., Huang, C., Vallyathan, V., Castranova, V. and Shi, X. (2003) Role of reactive oxygen species and MAPKs in vanadate-induced G(2)/M phase arrest. *Free Radic. Biol. Med.*, **34**, 1333–1342.
39) Abrieu, A., Doree, M. and Picard, A. (1997) Mitogen-activated protein kinase activation down-regulates a mechanism that inactivates cyclin B-cdc2 kinase in G2-arrested oocytes. *Mol. Biol. Cell.*, **8**, 249–261.
40) Park, J. S., Carter, S., Reardon, D. B., Schmidt-Ullrich, R., Dent, P. and Fisher, P. B. (1999) Roles for basal and stimulated p21(Cip-1/WAF1/MDA6) expression and mitogen-activated protein kinase signaling in radiation-induced cell cycle checkpoint control in carcinoma cells. *Mol. Biol. Cell.*, **10**, 4231–4246.
41) Mikkelsen, R. B. and Wardman, P. (2003) Biological chemistry of reactive oxygen and nitrogen and radiation-induced signal transduction mechanisms. *Oncogene*, **22**, 5734–5754.
42) Anderson, S., Bankier, A. T., Barrell, B. G., de Bruijn, M. H., Coulson, A. R., Drouin, J., Eperon, I. C., Nierlich, D. P., Roe, B. A., Sanger, F., Schreier, P. H., Smith, A. J., Staden, R. and Young, I. G. (1981) Sequence and organization of the human mitochondrial genome. *Nature* (London), **290**, 457–465.
43) Boveris, A. and Chance, B. (1973) The mitochondrial generation of hydrogen peroxide. General properties and effect of hyperbaric oxygen. *Biochem. J.*, **134**, 707–716.
44) Dey, R. and Moraes, C. T. (2000) Lack of oxidative phosphorylation and low mitochondrial membrane potential decrease susceptibility to apoptosis and do not modulate the protective effect of Bcl-x(L) in osteosarcoma cells. *J. Biol. Chem.*, **275**, 7087–7094.

Instructions for Authors

The Journal of Health Science is published by the Pharmaceutical Society of Japan, and covers all aspects of health science. The Journal will publish high quality original research related to health, as effected by nutrients, endogenous factors, chemicals (including drugs), and microorganisms, employing the techniques of biochemistry, molecular biology, toxicology, and epidemiology. Reports on analytical methods and experimental techniques are also within the scope of the Journal.

The Journal will accept original and innovative submissions in English from both members and non-members of the Pharmaceutical Society of Japan, on the understanding that the work is unpublished and is not being considered for publication elsewhere.

Types of Manuscript

The Journal publishes Regular Articles, Rapid Communications, Research Letters, Reviews and Minireviews. With the exception of Reviews and Minireviews, manuscripts will be reviewed by two or more referees, whose opinions will form the basis of the final decision by the Editor.

(1) *Regular Articles*

New, significant, innovative and original findings are suitable as *Regular Articles*. Whilst the Journal does not publish Short Communications, relatively short *Regular Articles* are also acceptable if the work is of a high quality.

(2) *Rapid Communications*

These articles should be 4 or less printed journal pages. Manuscripts are reviewed rapidly. Authors are informed of the editor's decision by FAX or E-mail within 2 weeks after reception of the manuscript. The editor's decision is either acceptance or rejection for publication, and no revision process will take place. Responsibility for the scientific contents of a manuscript remains with the author. In the case of rejection, a short explanation only will be provided. When submitting *Rapid Communications*, please include a floppy disk containing the text and any figures, tables etc.

(3) *Research Letters*

Research Letters should occupy 3 printed journal pages or less. Manuscripts containing interesting findings without adequate discussion, research results of narrow scope or of a predominantly negative nature may nevertheless be suitable for publication as a *Research Letter* if they are considered sufficiently important. Subjects of relevance to health science, for example DNA sequences of unknown genes and transcriptional regulation regions etc, are also suitable as *Research Letters*. Manuscripts containing valuable data obtained in field work are also acceptable. When it is necessary to present a relatively large amount of data in field work, the paper may extend to more than 3 printed pages.

(4) *Reviews and Minireviews*

Reviews and Minireviews are submitted by invitation from the Editorial Board, and encompass recent important scientific discoveries. *Minireviews* mainly involve a description of recent research results from the author's laboratory. *Reviews* are more broad based. Whilst *Reviews* do not have a page limit, *Minireviews* should be 3 pages or less of printed Journal space.

Submission of Manuscripts

Manuscripts (in triplicate) should be submitted to :

(From Japan)
Journal of Health Science Editorial Office
The Pharmaceutical Society of Japan
2-12-15, Shibuya, Shibuya-ku, Tokyo 150-0002, Japan

(From the rest of the world)
Dr. Y. James Kang
Associate Editor, Journal of Health Science
Department of Medicine,
University of Louisville School of Medicine
511 S. Floyd St., MDR 530, Louisville, Kentucky 40202, U.S.A.

Manuscript Preparation

(1) *Manuscript Form* : All manuscripts should be typewritten in English on A4 paper, double space (24 lines per page, approx. 70 strokes per line). Since after printing, one page contains about 4300 characters, please take care when preparing the paper to not exceed the allowed length for the specific type of manuscript. The top (title) page should be numbered 1 at the bottom center. All subsequent pages should be numbered consecutively.

(2) *Title Page* : The title page (page 1) should start with the title, name(s) of the author(s) and affiliation and mailing address. An asterisk (*) should be added to the right of the corresponding author's name. Below the authors address(es) should be included the type of manuscript (Regular Article, Research Letter etc.) and the corresponding author's name, address, telephone number, fax number, and E-mail address.

(3) *Summary and Keywords* : Page 2 should contain a summary of less than 250 words and 3 to 6 descriptive key words, listed in order of importance. The first 3 key words must be independent, as they will be used in a key-word combination in the index.

(4) *Main Text* : The main text should start from page 3 and be divided into the follow sections: Introduction, Materials and Methods, Results, Discussion, Acknowledgments, and References. It is also acceptable to merge the Results

with the Discussion in the form: Results and Discussion.

(5) *Abbreviations and Units* : Abbreviation must be spelled out in full at their initial appearance, followed by the abbreviation in parentheses. Thereafter, the abbreviation may be employed. The following units should be used: length (m, cm, mm, nm, μm, Å), mass (kg, g, mg, μg, ng, pg, mol, mmol), volume (l, ml, μl), time (sec, min, hr), temperature (°C), radiation (Bq, Ci, Sv, Gy), concentration (M, mM, mol/l, mmol/l, mg/ml, μg/ml, %, %(v/v), ppm, ppb).

(6) *Figures* : In principle, figures prepared by the author will be used in the printed version of the journal. All figures should be numbered consecutively with Arabic numbers, and figure titles and legends are to be typed consecutively on a separate sheet. All figures should be prepared on A4 paper, and the authors name should be added at the top of each page.

(7) *Tables* : Tables should be typed on A4 paper and numbered consecutively with Arabic numbers. Any explanations of data or methods in the table should be directly below the table.

(8) *References* : References should be placed and numbered in the order of appearance in the text. Each number is to be positioned after the last relevant word with a right-half parenthesis mark, and all references should be collected together at the end of the text. Abbreviations for Journals should conform to Chemical Abstracts nomenclature.

Examples of References are as follow :

1) Kubo, U., Hwang, G. H. and Suzuki, H. (2000) Cloning and functional characterization of copper transporter. *J. Health Sci.*, **46**, 135–140.

2) Albert, B. and Hardin, T. D. (1998) *Metal Toxicology in Mammals*, Madison Press, New York.

3) Meister, B., Revel, T. M. and Caprio, M. N. (1999) Molecular mechanism of cell death. In *Handbook of Health Science* (Clarke, A. and Young, T. A., Eds.), Carrie Press, Tokyo, pp.135–137.

(9) *Notes* : Notes should be given in parentheses at the appropriate place in the text. Footnotes are not permitted.

Ethics

In scientific investigations involving human subjects, experiments should be performed in accordance with the ethical standards formulated in the Helsinki Declaration of 1964 (revised in 2000, cf. http://ohsr.od.nih.gov/). Similarly, animal experiments should follow the ethical standards formulated in the guidelines issued by the Science and International Affairs Bureau of the Japanese Ministry of Education, Science, Sports and Culture, No.141, 1987: "Animal Experiments in Universities etc."

Page Charges

Authors are required to pay charges, as outlined below :

(1) Page Charge : 4000 yen per printed page (not including tax). Charges may be changed without prior notice.

(2) Reprint Charges are as undermentioned table.

(3) Color Figures : Actual cost.

(4) The payment of page charge is required, but is not a condition for publication, since the decision for publication is made on the basis of scientific significance only. The publication charge may be waived upon request from authors who do not have funds. No free reprints of the article are provided.

Miscellaneous

(1) Any author who is not fully fluent in idiomatic English is urged to gain assistance with manuscript preparation from an appropriate person who can check and improve the English of their paper.

(2) Rejected manuscripts will not be returned to the author.

(3) Revised manuscripts must be returned with 2 months, otherwise they will be treated as new submissions.

(4) Except for Rapid Communications, a floppy disk containing text and figure files must be sent with the revised manuscript.

(5) The author is given an opportunity to proof the galley of an accepted manuscript. Major changes at this time are not permitted.

(6) Copyrights : The copyrights of all manuscripts published in Journal of Health Science belong to the Pharmaceutical Society of Japan. The author must submit a Copyright Transfer form to the Pharmaceutical Society of Japan.

(http://jhs.pharm.or.jp)

Reprint Charges

Number of Pages / Number of Reprints	1~2	3~4	5~6	7~8	9~10	Greater than 11
50	¥ 8000	¥ 9000	¥ 10000	¥ 11000	¥ 12000	¥ 13000
100	¥ 14400	¥ 16200	¥ 18000	¥ 19800	¥ 21600	¥ 23400
150	¥ 19200	¥ 21600	¥ 24000	¥ 26400	¥ 28800	¥ 31200
200	¥ 22400	¥ 25200	¥ 28000	¥ 30800	¥ 33600	¥ 36400
More than 250	¥ 110 each	¥ 120 each	¥ 130 each	¥ 150 each	¥ 160 each	¥ 180 each

• Postage included ; Tax extra. • Color printing carries on extra surcharge of ¥80 per page.

• Reprints only available in multiples of 50.

Int. J. Cancer: **116,** 36–44 (2005)

Establishment of a human non-small cell lung cancer cell line resistant to gefitinib

Fumiaki Koizumi[1,3], Tatsu Shimoyama[1,4], Fumiko Taguchi[1,4], Nagahiro Saijo[2] and Kazuto Nishio[1,4]*
[1]*Shien-Lab, National Cancer Center Hospital, Tokyo, Japan*
[2]*Medical Oncology Department, National Cancer Center Hospital, Tokyo, Japan*
[3]*Investigative Treatment Division, National Cancer Center Research Institute EAST, Kashiwa, Japan*
[4]*Pharmacology Division, National Cancer Center Research Institute, Tokyo, Japan*

The epidermal growth factor receptor (EGFR) tyrosine-kinase inhibitor gefitinib (Iressa®, ZD1839) has shown promising activity preclinically and clinically. Because comparative investigations of drug-resistant sublines with their parental cells are useful approaches to identifying the mechanism of gefitinib resistance and select factors that determine sensitivity to gefitinib, we established a human non-small cell lung carcinoma subline (PC-9/ZD) that is resistant to gefitinib. PC-9/ZD cells are ~180-fold more resistant to gefitinib than their parental PC-9 cells and PC-9/ZD cells do not exhibit cross-resistance to conventional anticancer agents or other tyrosine kinase inhibitors, except AG-1478, a specific inhibitor of EGFR. PC-9/ZD cells also display significant resistance to gefitinib in a tumor-bearing animal model. To elucidate the mechanism of resistance, we characterized PC-9/ZD cells. The basal level of EGFR in PC-9 and PC-9/ZD cells was comparable. A deletion mutation was identified within the kinase domain of *EGFR* in both PC-9 and PC-9/ZD, but no difference in the sequence of *EGFR* cDNA was detected in either cell line. Increased EGFR/HER2 (and EGFR/HER3) heterodimer formations were demonstrated in PC-9/ZD cells by chemical cross-linking and immunoprecipitation analysis in cells unexposed to gefitinib. Exposure to gefitinib increased heterodimer formation in PC-9 cells, but not in PC-9/ZD cells. Gefitinib inhibits EGFR autophosphorylation in a dose-dependent manner in PC-9 cells but not in PC-9/ZD cells. A marked difference in inhibition of site-specific phosphorylation of EGFR was observed at Tyr1068 compared to other tyrosine residues (Tyr845, 992 and 1045). To elucidate the downstream signaling in the PC9/ZD cellular machinery, complex formation between EGFR and its adaptor proteins GRB2, SOS, and Shc was examined. A marked reduction in the GRB2-EGFR complex and absence of SOS-EGFR were observed in PC-9/ZD cells, even though the protein levels of GRB2 and SOS in PC-9 and PC-9/ZD cells were comparable. Expression of phosphorylated AKT was increased in PC-9 cells and inhibited by 0.02 μM gefitinib. But the inhibition was not significant in PC-9/ZD cells. These results suggest that alterations of adaptor-protein-mediated signal transduction from EGFR to AKT is a possible mechanism of the resistance to gefitinib in PC-9/ZD cells. These phenotypes including EGFR–SOS complex and heterodimer formation of HER family members are potential biomarkers for predicting resistance to gefitinib.

Key words: resistance; gefitinib; EGFR; Grb2; SOS; non-small cell lung cancer

Chemotherapy has played a central role in the treatment of patients with inoperable NSCLC for over 30 years, although its efficacy seems to be of very limited value.[1,2] Human solid tumors, including lung cancer, glioblastoma, breast cancer, prostate cancer, gastric cancer, ovarian cancer, cervical cancer and head and neck cancer, express epidermal growth factor receptor (EGFR) frequently, and elevated EGFR levels are related to disease progression, survival, stage and response to therapy.[2–10] The therapies directed at blocking EGFR function are attractive.

Interest in target-based therapy has been growing ever since the clinical efficacy of STI-571 was first demonstrated,[11–13] and small molecules and monoclonal antibodies that block activation of the EGFR and HER2 have been developed over the past few decades. The leading small-molecule EGFR tyrosine-kinase inhibitor, gefitinib (Iressa®, ZD1839), has shown excellent antitumor activity in a series of Phase I and II studies,[14,15] and Phase II international multicenter trials (Iressa Dose Evaluation in Advanced Lung Cancer (IDEAL) 1 and 2) yield an overall RR of 11.8–18.4% and overall disease control rate of 42.2–54.4% (gefitinib 250 mg/day) in patients with advanced non-small cell lung cancer (NSCLC) who had undergo at least 2 previous treatments with chemotherapy. INTACT 1 and 2 ('Iressa' NSCLC Trials Assessing Combination Therapy) have demonstrated that gefitinib does not provide improvement in survival when added to standard first line platinum-based chemotherapy *vs.* chemotherapy alone in advanced NSCLC.[16,17] Two small retrospective studies reported recently that activating mutation of *EGFR* correlate with sensitivity and clinical response to gefitinib and erlotinib.[18–20] Although information of *EGFR* mutation may enable to identify the subgroup of patients with NSCLC who will respond to gefitinib and erlotinib, it would be expected that acquired resistance would develop in such patients after treatment. The problem of acquired resistance to gefitinib might be growing, but there has been no preclinical research about the mechanism of developing resistance to gefitinib. We established resistant subline using PC-9 that is highly sensitive to gefitinib.

Establishment of drug-resistant sublines and comparative investigations with their parental cells to identify their molecular, biological and biochemical properties are useful approaches to elucidating the mechanism of the drug's action. Our study describes the establishment of a gefitinib-resistant cell line and its characterization at the cellular and subcellular levels. The PC-9/ZD cell line is the first human NSCLC cell line resistant to gefitinib ever reported. PC-9 is a lung adenocarcinoma cell line that is highly sensitive to gefitinib at its IC_{50}-value of 0.039 μM, but the PC-9/ZD subline, which has a level of EGFR expression comparable to that of PC-9 cells, is specifically resistant to gefitinib. Thus, PC-9 and PC-9/ZD cells will provide useful information about the mechanism of developing resistance to gefitinib and molecules as surrogate markers for predicting chemosensitivity to gefitinib.

Material and methods

Drugs and cells

Gefitinib(*N*-(3-chloro-4-fluorophenyl)-7-methoxy-6-[3-(morpholin-4-yl)propoxy] quinazolin-4-amine) was supplied by AstraZeneca Pharmaceuticals (Cheshire, UK). AG-1478, AG-825, K252a, staurosporin, genistein, RG-14620 and Lavendustin A were purchased from Funakoshi Co. Ltd (Tokyo, Japan).

NSCLC cell line PC-9 (derived from a patient with adenocarcinoma untreated previously) was provided by Prof. Hayata of Tokyo Medical University (Tokyo, Japan).[21] PC-9 and PC-9/ZD cells were cultured in RPMI-1640 medium (Sigma, St. Louis, MO) supplemented with 10% FBS (GIBCO-BRL, Grand Island, NY), penicillin and streptomycin (100 U/ml and 100 μg/ml, respectively; GIBCO-BRL) in a humidified atmosphere of 5%

***Correspondence to:** Shien-Lab, Medical Oncology Department, National Cancer Center Hospital, 5-1-1 Tsukiji, Chuo-ku, Tokyo, 104-0045, Japan. Fax: +81-3-3547-5185. E-mail: knishio@gan2.res.ncc.go.jp
Received 1 July 2004; Accepted after revision 21 December 2004
DOI 10.1002/ijc.20985
Published online 10 March 2005 in Wiley InterScience (www.interscience.wiley.com).

Publication of the International Union Against Cancer

CO_2 at 37°C. Gefitinib-resistant PC-9/ZD cells were selected from a subculture that had acquired resistance to gefitinib using the following procedure. Cultured PC-9 cells were exposed to 2.5 μg/ml *N*-methyl-*N'*-nitro-*N*-nitrosoguanidine (MNNG) for 24 hr and then washed and cultured in medium containing 0.2 μM gefitinib for 7 days. After exposure to gefitinib, they were washed and cultured in drug-free medium for 14 days. When variable cells had increased, they were seeded in medium containing 0.3–0.5 μM of gefitinib on 96-well cultured plates for subcloning. After 21–28 days, the colonies were harvested and a single clone was obtained. The subcloned cells exhibited an 182-fold increase in resistance to the growth-inhibitory effect of gefitinib as determined by MTT assay, and the resistant phenotype has been stable for at least 6 months under drug-free conditions.

In vitro *growth-inhibition assay*

The growth-inhibitory effects of cisplatin, carboplatin, adriamycin, irinotecan, gemcitabine, vindesine, paclitaxel, genistein, K252a, staurosporin, AG-825, AG-1478, Tyrophostin 51, RG-14620, Lavendustin A and gefitinib in PC-9 and PC-9/ZD cells were examined by using a 3-(4,5-dimethylthiazol-2-yl)- 2,5-diphenyltetrazolium bromide (MTT) assay.[22] A 180 μl volume of an exponentially growing cell suspension (6×10^3 cells/ml) was seeded into a 96-well microtiter plate, and 20 μl of various concentrations of each drug was added. After incubation for 72 hr at 37°C, 20 μl of MTT solution (5 mg/ml in PBS) was added to each well, and the plates were incubated for an additional 4 hr at 37°C. After centrifuging the plates at 200*g* for 5 min, the medium was aspirated from each well and 180 μl of DMSO was added to each well to dissolve the formazan. Optical density was measured at 562 and 630 nm with a Delta Soft ELISA analysis program interfaced with a Bio-Tek Microplate Reader (EL-340, Bio-Metallics, Princeton, NJ). Each experiment was carried out in 6 replicate wells for each drug concentration and carried out independently 3 or 4 times. The IC_{50}-value was defined as the concentration needed for a 50% reduction in the absorbance calculated based on the survival curves. Percent survival was calculated as: (mean absorbance of 6 replicate wells containing drugs − mean absorbance of six replicate background wells)/(mean absorbance of 6 replicate drug-free wells − mean absorbance of 6 replicate background wells) × 100.

In vivo *growth-inhibition assays*

Experiments were carried out in accordance with the United Kingdom Coordinating Committee on Cancer Research Guidelines for the welfare of animals in experimental neoplasia (2nd ed.). Female BALB/c nude mice, 6-weeks-old, were purchased from Japan Charles River Co. Ltd (Atsugi, Japan). All mice were maintained in our laboratory under specific-pathogen-free conditions. *In vivo* experiments were scheduled to evaluate the effect of oral administration of gefitinib on pre-existing tumors. Ten days before administration, 5×10^6 PC-9 or PC-9/ZD cells were injected subcutaneously (s.c.) into the back of the mice, and gefitinib (12.5, 25 or 50 mg/kg, p.o.) was administered to the mice on Days 1–21. Tumor diameter was measured with calipers on Days 1, 4, 8, 11, 14, 19 and 22 to evaluate the effect of treatment, and tumor volume was determined by using the following equation: tumor volume = $ab^2/2$ (mm^3) (where *a* is the longest diameter of the tumor and *b* is the shortest diameter). Day "x" denotes the day on which the effect of the drugs was estimated, and Day "1" denotes the first day of treatment. All mice were sacrificed on Day 22, after measuring their tumors. We considered absence of a tumor mass on Day 22 to indicate a cure. Differences in tumor sizes between the treatment groups and control group at Day 22 were analyzed by the unpaired *t*-test. A *p*-value of <0.05 was considered statistically significant.

cDNA expression array

The gene expression profile of PC-9/ZD was assessed with an Atlas Nylon cDNA Expression Array (BD Bioscience Clontech, Palo Alto, CA). Total RNA was extracted by a single-step guanidinium thiocyanate procedure (ISOGEN, Nippon Gene, Tokyo, Japan). An Atlas Pure Total RNA Labeling System was used to isolate RNA and label probes. The materials provided with the kit were used, and the manufacturer's instructions were followed for all steps. Briefly, streptavidin-coated magnetic beads and biotinylated oligo(dT) were used to isolate poly A RNA from 50 μg of total RNA and the RNA obtained was converted into ^{32}P-labeled first-strand cDNA with MMLV reverse transcriptase. The ^{32}P-labeled cDNA fraction was purified on NucleoSpin columns and was added to the membrane on which fragments of 777 genes were spotted. Hybridization was allowed to proceed overnight at 68°C. After washing, the radiolabeled spots were visualized and quantified by BAS-2000II and Array Gauge 1.1 (Fuji Film Co., Ltd., Tokyo, Japan). The data were adjusted for the total density level of each membrane.

Quantitative real-time RT-PCR analysis

Total RNAs extracted from PC-9 cells and PC-9/ZD cells (1×10^6 cells each) were incubated with DNase I (Invitrogen, Carlsbad, CA) for 30 min. First-strand cDNA synthesis was carried out on 1 μg of RNA in 10 μl of a reaction mixture with 50 pmol of Random hexamers and 50 U of M-MLV RTase. Oligonucleotide primers for human *EGFR* were obtained from Takara (HA003051, Takara Bio Co., Tokyo, Japan). For PCR calibration, we generated a calibrator dilution series for *EGFR* cDNA in pUSEamp vector (Upstate, Charlottesville, VA) ranging from 10^8–10^2 copies/1 μl. A total of 2 μl of reverse transcriptase products was used for PCR amplification using Smart Cycler system (Takara) according to manufacturer's instructions. Absolute copy numbers were calculated back to the initial cell numbers, which were set into the RNA extraction. As a result we obtained copies/cell:ratio representing the average *EGFR* RNA amount per cell.

Immunoprecipitation and immunoblotting

The cultured cells were washed twice with ice-cold PBS, and lysed in EBC buffer (50 mM Tris-HCl, pH 8.0, 120 mM NaCl, 0.5% Nonidet P-40, 100 mM NaF, 200 mM Na orthovanadate, and 10 mg/ml each of leupeptin, aprotinin, pepstatin A and phenylmethylsulphonyl fluoride). The lysate was cleared by centrifugation at 15,000 r.p.m. for 10 min, and the protein concentration of the supernatant was measured by BCA protein assay (Pierce, Rockford, IL). The membrane was probed with antibody against EGFR (1005; Santa Cruz, Santa Cruz, CA), HER2/neu (c-18; Santa Cruz), HER3 (c-17; Santa Cruz), HER4 (c-18; Santa Cruz), PI3K (4; BD), Grb2 (81; BD), SOS1/2 (D-21; Santa Cruz), Shc (30; BD, San Jose, CA), PTEN (9552; Cell Signaling, Beverly, MA), AKT (9272; Cell Signaling), phospho-EGFR specific for Tyr 845, Tyr 992, Tyr 1045, and Tyr 1068 (2231, 2235, 2237, 2234; Cell Signaling), phospho-AKT (Ser473) (9271; Cell Signaling), phospho-Erk (9106; Cell Signaling), and phospho-Tyr (PY-20; BD) as the first antibody, and then with by horseradish-peroxidase-conjugated secondary antibody. The bands were visualized by enhanced chemiluminescence (ECL Western Blotting Detection Kit, Amersham, Piscataway, NJ). For Immunoprecipitation, 5×10^6 cells were washed, lysed in EBC buffer, and centrifuged, and the supernatants obtained (1,500 μg) were incubated at 4°C with the anti-EGFR (1005), -HER2 (c-18), and -HER3 (c-17) Ab overnight. The immunocomplexes were absorbed onto protein A/G-Sepharose beads, washed 5 times with lysate buffer, denatured, and subjected to electrophoresis on a 7.5% polyacrylamide gel.

Analysis of the genes of the HER families by direct sequencing

Total RNAs were extracted from PC-9 and PC-9/ZD cells with ISOGEN (Nippon Gene) according to manufacturer's instructions. First-strand cDNA was synthesized from 2 μg of total RNA by using 400 U of SuperScript II (Invitrogen, Carlsbad, CA). After reverse transcription with oligo (dT) primer (Invitrogen) or random primer (Invitrogen), the first-strand cDNA was amplified by PCR by using specific primers for *EGFR*, *HER2* and *HER3*. The

reaction mixture (50 µl) contained 1.25 U AmpliTaq DNA polymerase (Applied Biosystem, Foster City, CA), and amplification was carried out by 30 cycles of denaturation (95°C, 30 sec), annealing (55–59°C, 30 sec), and extension (72°C, 30 sec) with a GeneAmp PCR System 9600 (Applied Biosystem). After amplification, 5 µl of the RT-PCR products was subjected to electrophoretic analysis on a 2% agarose gel with ethidium bromide. DNA sequencing of the PCR products was carried out by the dideoxy chain termination method using the ABI PRISM 310 Genetic Analyzer (Applied Biosystem).

Chemical cross-linking

Chemical cross-linking in intact cells was carried out as described previously.[23] In brief, after 6 hr exposure to 0.2 µM gefitinib, cells were washed with PBS and incubated for 25 min at 4°C in PBS containing 1.5 mM of the nonpermeable cross-linker bis (sulfosuccinimidyl) substrate (Pierce, Rockford, IL). The reaction was terminated by adding 250 mM glycine for 5 min while rocking. Cells were washed in EBC buffer and 20 µg of protein was resolved by 5–10% gradient SDS-PAGE, and then immunoblot analyzed for EGFR, HER2, HER3 and P-Tyr.

Results

Sensitivity of PC-9/ZD cells to cytotoxic agents and tyrosine kinase inhibitors

No significant difference between PC-9 and PC-9/ZD cells was observed in *in vitro* cell growth (doubling time of 20.3 hr and 21.4 hr, respectively) and microscopic morphology. Figure 1 shows the growth-inhibitory effect of gefitinib on the parent PC-9 cell line and its resistant subline, PC-9/ZD. The IC_{50}-value of gefitinib in PC-9 cells was 0.039 µM, as compared to 7.1 µM in PC-9/ZD cells (182-fold resistance). PC-9/ZD cells exhibited no cross-resistance to other conventional anticancer agents, including cisplatin, carboplatin, adriamycin, vindesine, paclitaxel and irinotecan. We also examined the growth-inhibitory effect of the EGFR tyrosine kinase inhibitors AG-1478, RG-14620 and Lavendustin A and other tyrosine kinase inhibitors in PC-9 and PC-9/ZD cells. PC-9/ZD cells show cross-resistance to AG1478, but not to all of the tyrosine kinase inhibitors (Tables I, II). It is likely that PC-9/ZD would also be resistant to EGFR-targeted quinazoline derivatives including gefitinib and erlotinib.[20]

PC-9/ZD cells show significant resistance to gefitinib in an in vivo *model*

To ascertain whether the resistance of PC-9/ZD occurs *in vivo*, we investigated the growth-inhibitory effect of gefitinib on PC-9 cells and PC-9/ZD cells in a xenotransplanted model. There was no significant difference in the size of the of PC-9 and PC-9/ZD cell tumor masses in nude mice before the start of gefitinib injection. Figure 2 shows the growth-inhibition curve of PC-9 (Fig. 2*a*) and PC-9/ZD (Fig. 2*b*) cells *in vivo* during the observation period. The PC-9 tumor masses decreased markedly in volume at all doses of gefitinib. In the 50 mg/kg/day p.o. group, the PC-9 masses were eradicated in all mice and did not regrow within the observation period. Growth of the PC-9/ZD masses, on the other hand, was inhibited by gefitinib administration in a dose-dependent manner, but significant tumor reduction was observed only in the 25 and 50 mg/kg/day groups, and the PC-9/ZD masses were not eradicated even in 50 mg/kg/day group. These results clearly demonstrate the significant *in vivo* resistance of PC-9/ZD cells to gefitinib.

Expression of HER family members and related molecules in PC-9 and PC-9/ZD cells

We examined the gene expression and protein levels of HER family members and related molecules by cDNA expression array (followed by confirmation using RT-PCR, data not shown) and immunoblotting. The ratios of the protein expression levels of PC-9 cells to PC-9/ZD cells almost paralleled the expression levels of their genes (Fig. 3*a*). The basal level of EGFR was comparable or slightly higher in PC-9/ZD cells (Fig. 3*a*,*b*), whereas the HER3 and AKT levels were lower in resistant cells.

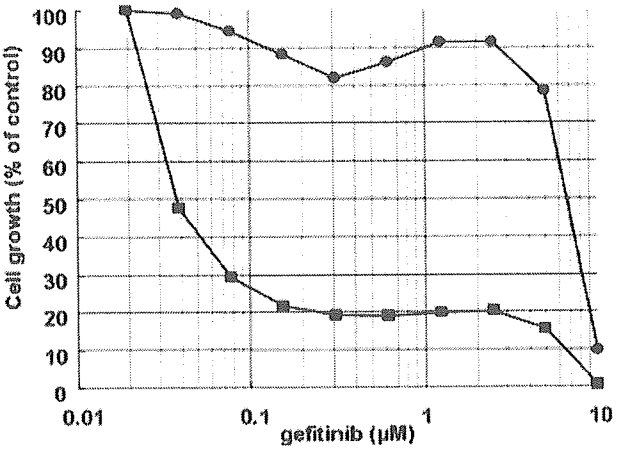

	PC-9	PC-9/ZD
IC_{50} value (µM)	0.039± 0.002	7.1± 0.06
Doubling time (hr)	20.3	21.0

FIGURE 1 – Growth-inhibitory effect of gefitinib on PC-9 and PC-9/ZD cells determined by MTT assay. The cells were exposed to the concentrations of gefitinib indicated for 72 hr. The growth–inhibition curves of PC-9 (■) and PC-9/ZD (●) are shown. Doubling time was determined by MTT assay.

TABLE I – CHEMOSENSITIVITY TO OTHER ANTICANCER DRUGS

Drug	IC_{50} values (µM)[1]		RR^2 1.6
	PC-9	PC-9/ZD	
Cisplatin	1.9 ± 0.7	3.1 ± 1.5	2.0
Carboplatin	25 ± 21	49 ± 23	1.3
Adriamycin	0.16 ± 0.13	0.20 ± 0.15	2.2
Irinotecan	15 ± 10	32 ± 11	1.5
Etoposide	4.5 ± 1.5	6.6 ± 1.3	1.5
Gemcitabine	18 ± 1.5	27 ± 1.5	0.7
Vindesine	0.0046 ± 0.0004	0.0032 ± 0.0009	1.2
Paclitaxel	0.0041 ± 0.0011	0.0048 ± 0.0004	1.6

[1]As assessed by MTT assay in PC-9 and PC-9/ZD cells. Values are the mean ± SD of >3 independent experiments.–[2]Relative resistance value (IC_{50} of resistant cells/IC_{50} of parental cells).

We carried out quantitative RT-PCR to measure the copy numbers of *EGFR*. Estimated transcript levels of *EGFR* were 786.3 and 712.1 copies/cell for PC-9 cells and PC-9/ZD cells, respectively (Fig. 3*d*). Relative ratio of *EGFR* expression levels in PC-9 cells and PC-9/ZD cells is 1.104. Microarray analysis using CodeLink Bioarray (Amersham Bio, Piscataway, NJ) confirmed equivalent gene expression of *EGFR* with ratio of 1.002 between PC-9 and PC-9/ZD cells (data not shown).

Expression of PI3K, Grb2, SOS, and Shc, the adaptor proteins of EGFR, and PTEN was almost the same in PC-9 and PC-9/ZD cells, and no change in the protein levels was observed after exposure to gefitinib (data not shown). The relative densitometric units of each protein are shown in Figure 3*c*. These results suggest that the difference in protein levels of EGFR, HER2, and related proteins can not explain the high resistance of PC-9/ZD cells to gefitinib.

Sequence of HER family member in PC-9/ZD cells

Several reports suggest that the resistance to receptor tyrosine kinase inhibitor STI-571 is partially due to mutations in the

TABLE II – CHEMOSENSITIVITY TO PROTEIN KINASE INHIBITORS[1]

Inhibitor	Target	IC_{50} values (μM)		RR[2]
		PC-9	PC-9/ZD	
AG-1478	EGFR	0.052 ± 0.02	6.0 ± 0.8	117
RG-14620	EGFR	13 ± 1.0	13 ± 2.5	1.0
Lavendustin A	EGFR	20 ± 4.6	27 ± 2.6	1.3
Genistein	TK	18 ± 1.5	27 ± 1.5	1.5
K252a	PKC	0.47 ± 0.17	0.63 ± 0.04	1.3
Staurosporin	PKC	0.0036 ± 0.0019	0.004 ± 0.0014	1.1
AG-825	HER2	>50	>50	

[1]Assessed by MTT assay in PC-9 and PC-9/ZD cells. Values are the mean ± SD of >3 independent experiments.–[2]Relative resistance value (IC_{50} of resistant cells/IC_{50} of parental cells).

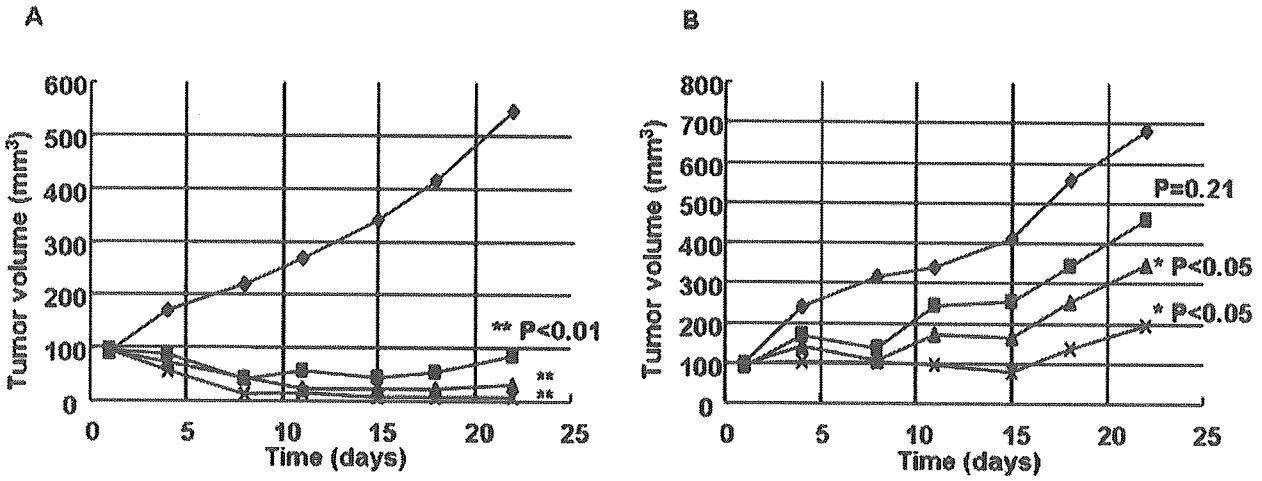

FIGURE 2 – Growth-inhibitory effect of gefitinib on PC-9 and PC-9/ZD cells xenotransplanted into nude mice. Ten days before gefitinib administration, 5 × 10^6 PC-9 (*a*) or PC-9/ZD (*b*) cells were injected s.c. into the back of mice. The mice were divided into 4 groups (◆, control group; ■, 12.5 mg/Kg group; ▲, 25 mg/Kg group; ×, 50 mg/Kg group). Gefitinib was administered p.o. to the tumor-inoculated mice on Days 1–21. Each group consisted of 6 mice. The statistical analysis was carried out by using the unpaired *t*-test.

ATP-binding site of the Bcr-Abl, the target of the drug.[24–27] We analyzed the sequences of the cDNAs of *EGFR*, *HER2*, and *HER3*, but found no differences in their sequences between PC-9 and PC-9/ZD cells. We did detect a deleted position of *EGFR* in both cell lines that results in deletion of 5 amino acids (Glu722, Leu723, Arg724, Glu725, and Ala726) (Fig. 4). Our findings indicate that the deletion does not directly contribute to the cellular resistance.

Inhibitory effect of gefitinib on autophosphorylation of EGFR in PC-9/ZD cells

Phosphorylation of EGFR is necessary for EGFR-mediated intracellular signaling. Although the EGFR phosphorylation levels of tumors were thought to be correlated with sensitivity to gefitinib, the basal level of phosphorylated EGFR in PC-9 and PC-9/ZD cells is almost the same. Gefitinib inhibited EGFR autophosphorylation in a dose-dependent manner and completely inhibited its phosphorylation at 0.2–2 μM in PC-9 cells (Fig. 5*a*), but its inhibitory effect on autophosphorylation of EGFR in PC-9/ZD cells was less than in PC-9 cells (Fig. 5*a*). Because each phosphorylation site of EGFR has a different role in the activation of downstream signaling molecules, we examined the inhibitory effect of gefitinib on site-specific phosphorylation of EGFR. Phosphorylation of several different EGFR tyrosine residues (Tyr845, Tyr992 and Tyr1068) was dose-dependently inhibited by gefitinib in PC-9 cells, whereas no clear inhibitory effects of gefitinib on phosphorylation at Tyr 845 and Tyr1068 residues in PC-9/ZD cells was observed (Fig. 5*b*,*c*,*e*). The most marked difference of in inhibition between the cells was observed at Tyr1068 (Fig. 5*e*). Tyr1045 showed resistance to inhibition of autophosphorylation by gefitinib in both PC-9 and PC-9/ZD cells (Fig. 5*d*).

Complex formation of EGFR and its adaptor proteins

Tyr1068 of EGFR is the tyrosine that is most resistant to inhibition of autophosphorylation by gefitinib in PC-9/ZD cells. Because the Tyr 1068 is a direct binding site for the GRB2/SH2 domain, and its phosphorylation is related to the complex formation of EGFR-adaptor proteins and their signaling, we examined complex formation between EGFR and the adaptor proteins GRB2, SOS, Shc, and PI3K by immunoprecipitation. The level of expression of these proteins in PC-9 and PC-9/ZD cells were similar (Fig. 3*a*). A smaller amount of EGFR-GRB2 complex was observed in PC-9/ZD cells and no EGFR-SOS complex was detected at all (Fig. 6). The amount of HER2- or HER3-GRB2 complex in PC-9 and PC-9/ZD cells was similar, and no decreases in complex formation were observed after exposure to gefitinib. A decreased amount of HER2-SOS complex and inability to detect HER3-SOS complex were also observed in PC-9/ZD cells. HER2-PI3K complex increased in PC-9/ZD. There are no significant differences in complex formation between SHC and EGFR, HER2, or HER3 between PC-9 and PC-9/ZD cells. These results suggest that GRB2-SOS-mediated signaling may be inactivated in PC-9/ZD cells.

Heterodimerization of HER family member in PC-9/ZD cells

Dimerization of members of the HER family is essential for activation of their catalytic activity and their signaling. We examined the effect of gefitinib on the dimerization of HER family members by immunoblotting, immunoprecipitation and chemical cross-linking analysis (Figs. 3*a*, 5*a*, 7*a*). The expression levels of EGFR and HER2 were similar and the HER3 level was lower in PC-9/ZD cells by immunoblotting (Fig. 3*a*). A chemical cross-

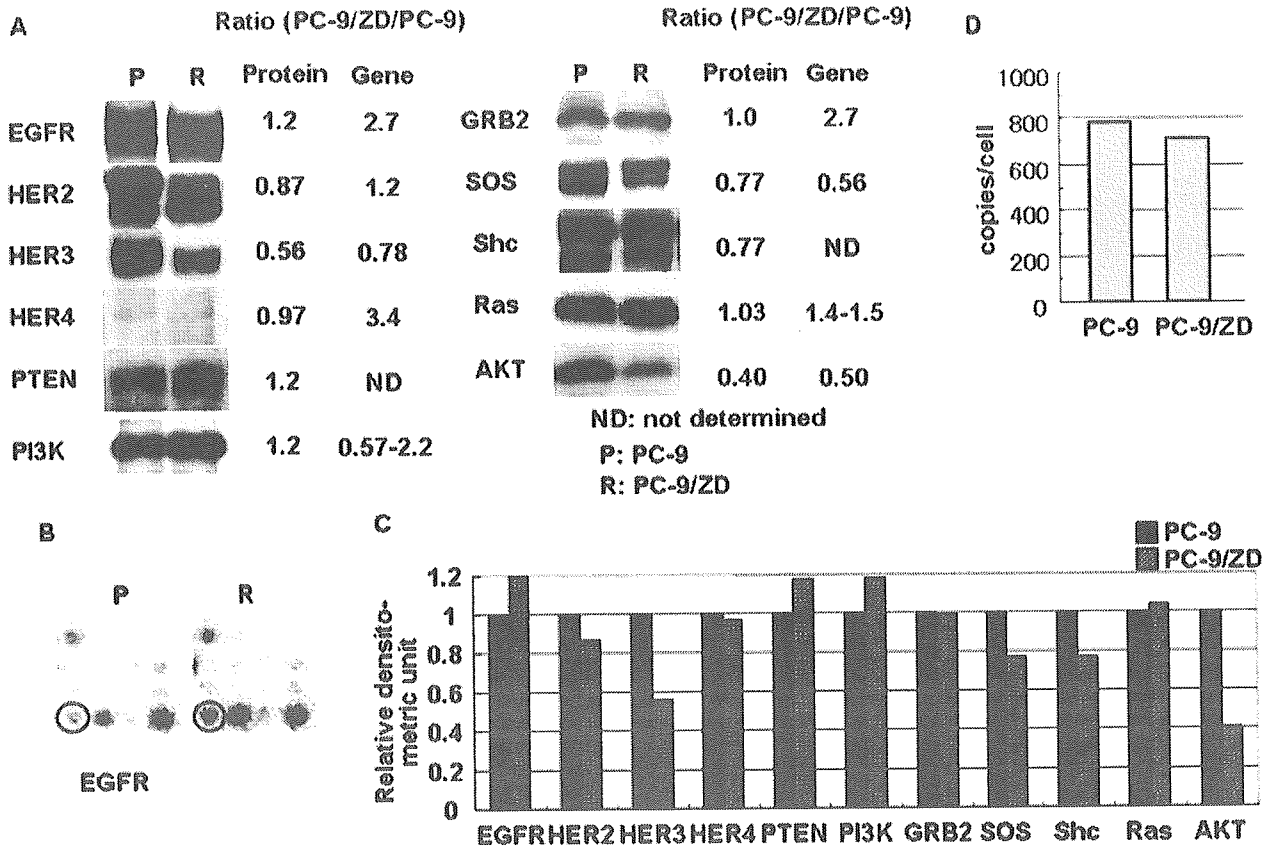

FIGURE 3 – Expresssion of HER family members and related molecules in PC-9 (P) and PC-9/ZD (R) cells. (*a*) Western blot analysis; a 20 μg sample of total cell lysates was separated by SDS-PAGE, transferred to a PVDF membrane, and incubated with a specific anti-human antibody as the first antibody and then with horseradish peroxidase-conjugated secondary antibody. The ratios of the levels of expression of proteins and genes in PC-9 cells to the levels in PC-9/ZD cells are shown. (*b*) cDNA expression array; Poly A RNA was converted into ^{32}P-labeled first-strand cDNA with MMLV reverse transcriptase. The ^{32}P-labeled cDNA fraction was hybridized to the membrane on which fragments of 777 genes were spotted. The close-up view shows *EGFR* mRNA expression. (*c*) Each band was quantified by a densitometry and with NIH image software. The levels of protein expression are shown in a graph. (*d*) Absolute amounts of *EGFR* transcripts of PC-9 cells and PC-9/ZD cells measured by real-time quantitative RT-PCR. The values were calculated back to the initial cell numbers for RNA extraction in Material and Methods.

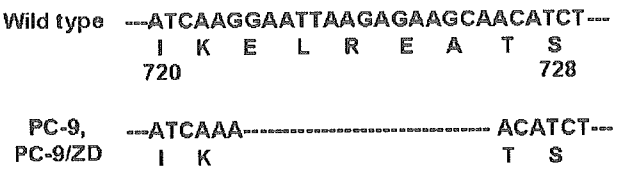

FIGURE 4 – Detection of a deleted position of EGFR. Direct sequencing of a PC-9 and PC-9/ZD-derived, amplified cDNA fragment containing the ATP-binding site of EGFR. *Top*, wild-type EGFR; *bottom*, PC-9 and PC-9/ZD.

linking assay showed that in the absence of gefitinib the amount of high molecular weight complexes (~400 kDa) that are recognized by anti-EGFR antibody (EGFR dimers), including formations of homodimers and heterodimers (EGFR-EGFR, EGFR-HER2 or EGFR-HER3), was almost the same in PC-9 and PC-9/ZD cells, whereas HER2 dimerization detected by anti-HER2 antibody was remarkably lower in PC-9/ZD cells (Fig. 7*a*). Increased EGFR/HER2 (and EGFR/HER3) heterodimer formation was detected in PC-9/ZD cells by immunoprecipitation analysis (Fig. 5*a*). The proportion of EGFR heterodimer to homodimer is increased significantly in PC-9/ZD (Fig. 7*b*). When exposed to gefitinib at a concentration of 0.2 μM for 6 hr the amount of dimer-formation increased similarly in PC-9 and PC-9/ZD cells (Fig. 7*a*), whereas marked induction of hetero-dimerization of EGFR-HER2 was observed only in PC-9 cells (Fig. 5*a*). These results suggest that a difference in hetero- or homo-dimerization is a possible determinant factor of gefitinib sensitivity.

AKT and MAPK pathways in PC-9/ZD cells

Because phosphorylation at Tyr 1068 of EGFR plays an important role for transduction of the signal to downstream of MAPK and AKT pathway,[28,29] we examined the difference between PC-9 and PC-9/ZD cells in downstream signaling. The basal level of phosphorylated AKT is higher in PC-9 cells than in PC-9/ZD cells, and although gefitinib inhibited AKT phosphorylation in a dose-dependent manner (Fig. 8*a*), the inhibitory effect of gefitinib on phosphorylation of AKT in PC-9/ZD cells was significantly less than in PC-9 cells (Fig. 8*a*). This difference in the inhibitory effect of gefitinib on AKT phosphorylation between PC-9 and PC-9/ZD cells is very similar to the difference in effect on EGFR autophosphorylation. No inhibition of phosphorylation of MAPK by gefitinib was observed in either cell line (Fig. 8*b*). These results suggest that downregulation of activated AKT is closely correlated with the cellular sensitivity to gefitinib, but that inhibition of the MAPK pathway does not contribute to drug sensitivity.